

Photochemical Removal of NO, NO₂, and N₂O by 146 nm Kr₂ Excimer Lamp in N₂ at Atmospheric Pressure

Masaharu Tsuji,^{*1,2} Naohiro Kamo,² Takashi Kawahara,² Masashi Kawahara,² Makoto Senda,² and Nobuyuki Hishinuma³

¹Institute for Materials Chemistry and Engineering, Kyushu University, Kasuga 816-8580

²Department of Applied Science for Electronics and Materials, Graduate School of Engineering Sciences, Kyushu University, Kasuga 816-8580

³USHIO Inc., Himeji 671-0224

Received September 1, 2008; E-mail: tsuji@cm.kyushu-u.ac.jp

The photochemical removal of NO, NO₂, and N₂O was investigated in N₂ using a 146 nm Kr₂ (25 mW cm⁻²) excimer lamp. The results obtained were compared with those obtained using 172 nm Xe₂ (50 or 300 mW cm⁻²) excimer lamps. The removal rates of NO and NO₂ at 146 nm were 11 and 36% slower than those at 172 nm, respectively. On the other hand, the removal rate of N₂O at 146 nm was 21 times faster than that at 172 nm. The differences in the removal rates are discussed in terms of the absorption coefficient at each wavelength and effects of photoabsorption by N₂ at 146 nm. By the addition of a small amount of O₂ into an N₂O/N₂ mixture, the removal rate of N₂O at 146 nm decreased greatly. On the basis of these facts, it was concluded that the 146 nm excimer lamp is especially useful for the N₂O removal in N₂ at atmospheric pressure.

Nitrogen oxides (NO_x: NO and NO₂), which arise from various industrial sources, are major contributors to acid rain.^{1,2} On the other hand, nitrous oxide (N₂O) in the Earth's atmosphere is a major contributor to the greenhouse effect due to its long atmospheric residence time of 120 years and its 310 times larger radiative forcing than that of CO₂.^{1,3,4} Removal methods of NO_x and N₂O using rare metal catalysts have been extensively studied and widely applied as aftertreatment techniques in automobiles and thermal power plants.^{5–9} Recently, the cost of rare metal catalysts has increased greatly because of economic growth in developing countries. Therefore, a new low-cost and catalyst-free aftertreatment process must be developed to overcome this problem.

We have recently initiated development of photochemical methods as a new promising removal method of NO, NO₂, and N₂O at atmospheric pressure without using expensive catalysts.^{10–17} At first, we studied the decomposition of NO₂ and N₂O using a 193 nm ArF excimer laser in N₂ at atmospheric pressure.^{10–13} It was found that 86% of NO₂ was converted to N₂, O₂, and NO after 3 min laser irradiation and the formation ratios of N₂, O₂, and NO, defined as [product gas]/[NO₂]₀, were 32, 75, and 22%, respectively.¹¹ N₂O was nearly completely converted to N₂ and O₂ after 20 min laser irradiation.¹³ An advantage of the photochemical method is that N₂ is inert to photoirradiation above the 150 nm range. Therefore, NO emission due to the decomposition of N₂, which generally occurs in an electric discharge of N₂/O₂ mixtures,¹⁸ is negligible. However, when the ArF excimer laser photolysis is applied to practical NO_x removal, there are many severe problems such as the expense of the excimer laser apparatus,

the high running cost, and the large size and heavy weight of the apparatus including high-power sources. Another disadvantage is that NO, which is generally emitted in exhausted gases, cannot be removed efficiently. This is because the dissociation energy of NO (6.50 eV) is higher than that of the photon energy of ArF laser (6.43 eV).^{19,20}

In order to overcome these problems, we used a low-cost and compact 172 nm Xe₂ excimer lamp as a new vacuum ultraviolet (VUV) light source. Since the photon energy of 172 nm (7.21 eV) is higher than the dissociation of NO, not only the decomposition of NO₂ and N₂O but also that of NO is energetically possible. We have recently studied the removal of NO, NO₂, and N₂O using 172 nm Xe₂ excimer lamps (50 and 300 mW cm⁻²) in N₂ and N₂/O₂ mixtures.^{14–17}

In the present study, we studied the photochemical removal of NO, NO₂, and N₂O in N₂ using a 146 nm Kr₂ excimer lamp as an additional VUV source for the removal of these molecules. In Table 1 are summarized absorption cross sections of NO, NO₂, N₂O, N₂, and O₂ at 146 and 172 nm denoted as σ_{146} and σ_{172} , respectively, and their ratios, $\sigma_{146}/\sigma_{172}$. The $\sigma_{146}/\sigma_{172}$ ratios of NO, NO₂, and N₂O are 80, 0.93, and 65, respectively. Although there is no absorption of N₂ at 172 nm, N₂ absorbs 146 nm light. On the basis of these facts, higher removal rates are expected for NO and N₂O at 146 nm, if the absorption of the buffer N₂ gas at 146 nm does not interfere with the removal of these molecules. The removal rates of each gas and the formation ratios of products at 146 nm were compared with those at 172 nm. Possible removal mechanisms of NO, NO₂, and N₂O under VUV photoirradiation are discussed using reported photochemical and gas-phase kinetic data.^{19–23}

Table 1. Absorption Cross Sections of NO, NO₂, N₂O, N₂, and O₂ at 146 and 172 nm (Ref. 19) and Their Ratios

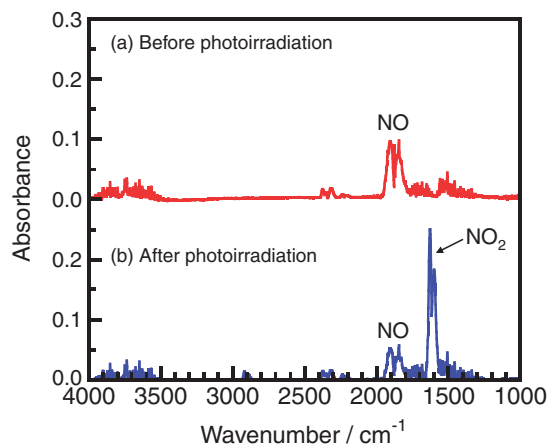
Molecules	Cross sections at 146 nm (σ_{146}) /cm ² molecule ⁻¹	Cross sections at 172 nm (σ_{172}) /cm ² molecule ⁻¹	$\sigma_{146}/\sigma_{172}$
NO	4×10^{-18}	5×10^{-20}	80
NO ₂	1.4×10^{-17}	1.5×10^{-17}	0.93
N ₂ O	6.5×10^{-18}	1.0×10^{-19}	65
N ₂	3.3×10^{-21}	0	
O ₂	1.5×10^{-17}	4.6×10^{-19}	33

Experimental

The VUV photolysis apparatus used in this work was the same as those reported previously.^{14–17} The inside volume of the photolysis chamber was 185 cm³. Lights from an unfocused 146 nm Kr₂ lamp (USHIO, UER20H146: 25 mW cm⁻², 120–165 nm range, full width at half maximum (FWHM): 16 nm) and 172 nm Xe₂ lamps (USHIO, UER20H172: 50 mW cm⁻² or USHIO trial product: 300 mW cm⁻² 155–200 nm range, FWHM: 14 nm) were used to remove NO, NO₂, and N₂O at room temperature. The diameter and length of the low power commercial Kr₂ and the Xe₂ lamps were 30 and 200 mm, whereas those of the high power Xe₂ lamp were 70 and 240 mm, respectively.

Experiments were carried out in a closed batch system. The total pressure was maintained at atmospheric pressure. The concentration of NO and NO₂ in pure N₂ was 1000 ppm (v/v), whereas that of N₂O in N₂ was 100 ppm. They were introduced through mass flowmeters. Before and after photoirradiation, outlet gases were analyzed using a HORIBA gas analysis system (FG122-LS) equipped with an FTIR spectrometer and an ANELVA gas analysis system (M-200GA-DTS) equipped with a quadrupole mass spectrometer. The detection limit of gases by the mass spectrometer was $\approx 0.1\%$. The lowly sensitive mass spectrometer was used for the determination of N₂/O₂ ratios of buffer gases, whereas the highly sensitive FTIR system was used for the detection of NO_x, N₂O, and O₃. The light path length and the volume of analyzing chamber in FTIR were 2.4 m and 300 cm³, respectively. The spectra were measured in the 900–5000 cm⁻¹ region with an optical resolution of 4 cm⁻¹. The reliable calibration curves of NO, NO₂, and N₂O for FTIR measurements were supplied by HORIBA Inc. The detection limits of NO₂, NO, and N₂O were, 1, 1, and ≈ 0.5 ppm, respectively, in our FTIR spectrometer. The concentration of O₃ was evaluated from the absorbance of O₃ by reference to standard spectral data supplied by HORIBA Inc. We determined the residual amount of a reagent gas A, $[A]/[A]_0$, and the formation ratio of a product gas B, $[B]/[A]_0$, from gas analysis. Here, $[A]_0$ is an initial concentration of A. The fluxes of photons in our 25 mW cm⁻² 146 nm and 50 mW cm⁻² 172 nm lamps were estimated to be 1.8×10^{16} and 4.3×10^{16} photons cm⁻² s⁻¹, respectively, indicating that the photon flux of the 146 nm lamp is smaller than that of the 172 nm one by a factor of 2.4. When the removal rates of NO₂, NO, and N₂O using the two lamps are compared, they are normalized to these photon fluxes of the lamps.

IR inactive N₂ and O₂ molecules could not be detected using the FTIR spectrometer. Therefore, no information could be obtained about concentrations of N₂ and O₂ from FTIR measurements. However, it was possible to evaluate the formation ratios of N₂ and O₂ from mass balance of N or O atom between reagent and products on the basis of gas-phase reactions shown later, when no products other than N₂O, NO, and NO₂ were obtained.

**Figure 1.** FTIR spectra of NO (1000 ppm) in N₂ (a) before and (b) after 25 mW cm⁻² Kr₂ excimer lamp irradiation for 30 min.

The following gases were used without further purification: N₂ (Taiyo Nissan Inc.: purity >99.9998%), NO (Taiyo Sanso Inc.: 2.02% in high purity N₂), NO₂ (Nippon Sanso Inc.: 3630 ppm in high purity N₂), N₂O (Nippon Sanso Inc.: 959 ppm in high purity N₂), and O₂ (Nippon Sanso Inc.: >99.99995%). NO and NO₂ in N₂ and N₂O in N₂ or N₂/O₂ mixtures were diluted before use.

Results and Discussion

NO Removal in N₂. Figures 1a and 1b show FTIR spectra of NO (1000 ppm) before and after 146 nm photoirradiation. After photoirradiation for 30 min, an NO peak at ≈ 1900 cm⁻¹ decreases in intensity by $\approx 50\%$, and an NO₂ peak at 1620 cm⁻¹ appears. The intensity of the NO₂ peak is ≈ 4 times stronger than that of the NO one in Figure 1b because the absorption peak of NO₂ at 1620 cm⁻¹ is about one order stronger than that of NO at ≈ 1900 cm⁻¹ at the same concentration. Similar FTIR spectra of NO were obtained after 172 nm photoirradiation. Figures 2a and 2b show the dependence of the residual amount of NO and the formation ratios of NO₂, N₂, and O₂ on the irradiation time of 25 mW cm⁻² 146 nm Kr₂ and 50 mW cm⁻² 172 nm Xe₂ lamps, respectively. The residual amount of NO at 146 nm decreases to 60, 48, and 34% with increasing the irradiation time to 10, 20, and 30 min, respectively. On the other hand, that at 172 nm decreases to 37, 12, and 9% for the same irradiation times. The formation ratio of NO₂ at 146 nm is about 20% in the 10–30 min range, whereas that at 172 nm is less than 10% in the same time range.

The removal rates of NO under 146 and 172 nm photoirradiation were determined assuming that they obey the following simple first-order decay of molecules.



$$[\text{NO}] = [\text{NO}]_0 \exp(-k_1 t) \quad (2)$$

The k_1 values of NO were evaluated to be 5.4×10^{-4} s⁻¹ at 146 nm and 1.4×10^{-3} s⁻¹ at 172 nm from slopes of plots of $\ln([\text{NO}]/[\text{NO}]_0)$ vs. irradiation time in the 0–30 min range. The correlation kinetic coefficients (R^2) of k_1 values in the linear least square plots were 0.949 at 146 nm and 0.962 at 172 nm. It is therefore reasonable to assume that the removal rates of NO obey a simple first order. Taking photon fluxes of the two lamps

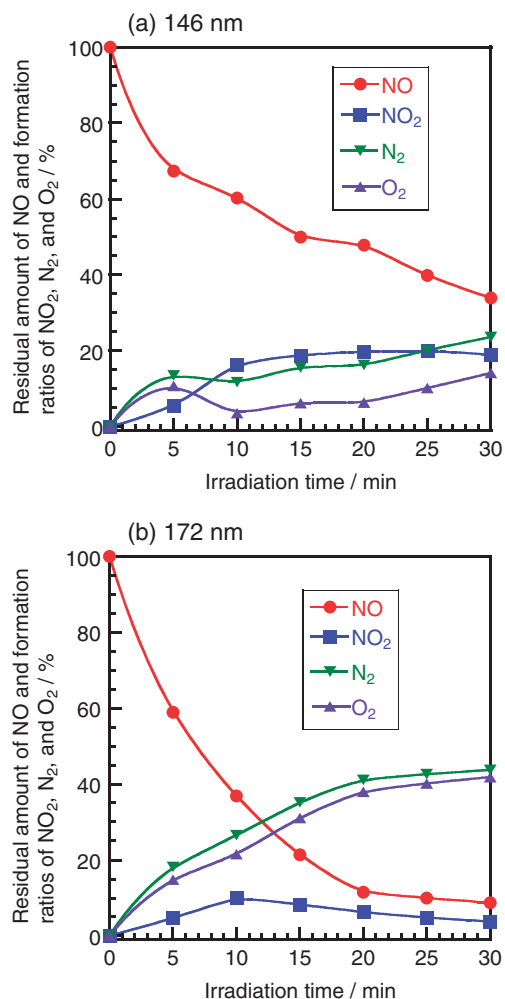


Figure 2. Dependence of the residual amount of NO and the formation ratios of NO₂, N₂, and O₂ on the irradiation time in N₂, when (a) 25 mW cm⁻² Kr₂ and (b) 50 mW cm⁻² Xe₂ excimer lamps were used. The formation ratios of N₂ and O₂ were obtained from mass balance. The initial NO concentration was 1000 ppm.

into account, the removal rate of NO at 146 nm is 11% slower than that at 172 nm. The absorption cross section of NO at 146 nm is 80 times larger than that at 172 nm (Table 1). Therefore, it is expected that the removal rate of NO at 146 nm is much faster than that at 172 nm, assuming that the removal rate of NO is governed by the absorption cross section of NO at different wavelengths. However, we found that the removal rate of NO at 146 nm is 11% slower than that at 172 nm. At 172 nm there is no absorption of N₂, whereas N₂ absorbs 146 nm light (Table 1). Thus, we estimated the contribution of absorption by the N₂ buffer gas using known absorption cross sections and concentrations of each gas.

In general, the total photon energy absorbed by such a mixture as NO and N₂ during passing through the decomposition chamber, E_{total} , is given by the relation:

$$E_{\text{total}} = E_0 - E_0 \exp\left(-l \sum_i \sigma_i N_i\right) \quad (3)$$

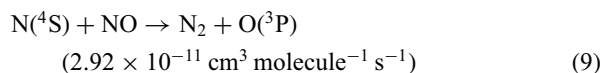
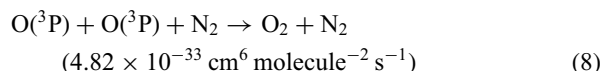
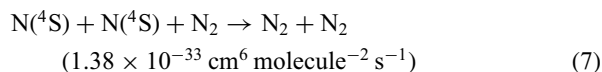
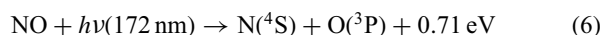
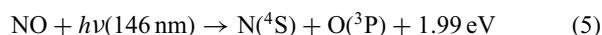
Here, E_0 , l , σ_i , and N_i are the energy of the excimer lamp, the

length of the decomposition chamber, the absorption cross section of a molecule i , and its number density, respectively. The photon energy absorbed by a molecule i , E_i , is obtained from the relation:

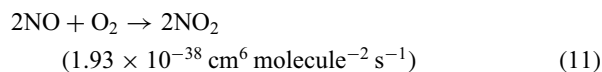
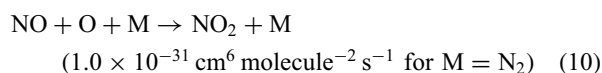
$$E_i = E_{\text{total}} \times \frac{\sigma_i N_i}{\sum_i \sigma_i N_i} \quad (4)$$

Although the σ_{N_2} value at 146 nm is three or four orders of magnitude smaller than NO, NO₂, and N₂O (Table 1), the N_{N_2} is 10³–10⁴ times larger than N_{NO_x} and $N_{\text{N}_2\text{O}}$. Therefore, the absorption of 146 nm light by N₂ may participate in the photolysis. When we calculated $E_{\text{NO}}/(E_{\text{NO}} + E_{\text{N}_2})$ and $E_{\text{N}_2}/(E_{\text{NO}} + E_{\text{N}_2})$ values at 146 nm using known σ_i and N_i values, they were 55 and 45%, respectively. These values suggest that one reason for the slow decomposition rate of NO at 146 nm is the absorption of 146 nm light by the buffer N₂ gas. Although N₂ absorbs about half of the 146 nm light, the decomposition rate of NO at 146 nm is expected to be still 44 times faster than that at 172 nm. Thus, another reason must be present for the slow removal rate of NO at 146 nm. The absorption spectrum of NO in the 130–200 nm range consists of many discrete bands.¹⁹ The Kr₂ lamp fits a sharp absorption peak of NO at 146 nm ($\sigma = 4 \times 10^{-18}$ cm² molecule⁻¹). On the other hand, the absorption cross section of NO at 172 nm is small ($\sigma = 5 \times 10^{-20}$ cm² molecule⁻¹). However, there are many other strong absorption peaks in the 155–200 nm region of the Xe₂ lamp and the maximum absorption cross section of such peaks is 1.6×10^{-18} cm² molecule⁻¹. Some of these strong absorption peaks may also contribute to the fast decomposition of NO using the 172 nm lamp, so that the removal rate of NO using 172 nm lamp is faster than expected from its small absorption cross section at 172 nm.

On the basis of FTIR data, the most probable formation processes of N₂ and O₂ from NO are VUV photolysis of NO (reactions 5 and 6) followed by secondary reactions 7–9.^{19–22}



On the other hand, NO₂ is produced through the following three-body reactions.^{20,21}



The formation ratio of NO₂ at 146 nm is larger than that at 172 nm. A major reason for the higher formation ratio of NO₂ is that the removal rate of NO₂ at 146 nm is slower than that at 172 nm by a factor of 3.7, as shown in the next section.

NO₂ Removal in N₂. Figures 3a and 3b show FTIR spectra

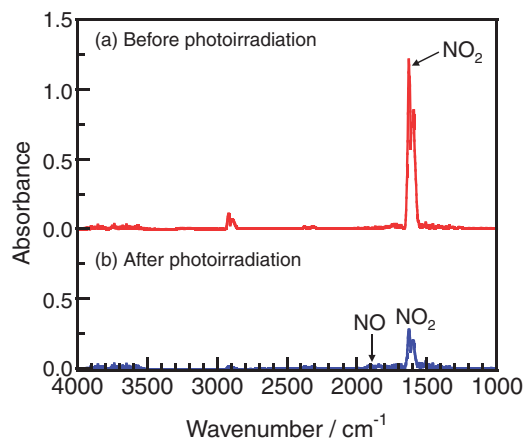


Figure 3. FTIR spectra of NO₂ (1000 ppm) in N₂ (a) before and (b) after 25 mW cm⁻² Kr₂ excimer lamp irradiation for 30 min.

of NO₂ (1000 ppm) before and after 146 nm photoirradiation, respectively. After photoirradiation for 30 min, an NO₂ peak at 1620 cm⁻¹ decreases in intensity by 80%. Similar FTIR spectra of NO₂ were obtained after 172 nm photoirradiation. Figure 4a shows the dependence of the residual amount of NO₂ and the formation ratios of NO, N₂, and O₂ on the irradiation time for the 25 mW cm⁻² 146 nm Kr₂ lamp. For comparison, corresponding data for the 50 mW cm⁻² 172 nm Xe₂ lamp are shown in Figure 4b.¹⁵ The residual amount of NO₂ at 146 nm decreases to 46, 28, and 19% with increasing irradiation time to 10, 20, and 30 min, respectively. On the other hand, that at 172 nm rapidly decreases to 13, 8, and 7% for the same irradiation times. Assuming first-order decay of NO₂, the removal rates of NO₂ at 146 and 172 nm, k_2 , were determined to be 9.0×10^{-4} and 3.3×10^{-3} s⁻¹ from slopes of plots of $\ln([\text{NO}_2]/[\text{NO}_2]_0)$ vs. irradiation time in the 0–10 min range at 146 nm and 0–30 min range at 172 nm. The correlation kinetic coefficients (R^2) of k_2 values in the linear plots were 0.977 at 146 nm and 0.951 at 172 nm. The correlation kinetic coefficients (R^2) of the k_2 value in the linear plot at 146 nm was 0.787 in the 0–30 min range, so we used values in the 0–10 min range giving the much better R^2 value shown above. Taking photon fluxes of the two lamps into account, the removal rate of NO₂ at 146 nm is 36% slower than that at 172 nm.

The absorption cross section of NO₂ at 146 nm is 7% smaller than that at 172 nm. When the $E_{\text{NO}_2}/(E_{\text{NO}_2} + E_{\text{N}_2})$ and $E_{\text{N}_2}/(E_{\text{NO}_2} + E_{\text{N}_2})$ values are evaluated using eq 4 and known σ_i and N_i values, they are 81 and 19%, respectively. These values suggest that the contribution of absorption by N₂ is smaller than that in the case of NO. The slower removal rate of NO₂ at 146 nm than that at 172 nm is consistent with the difference in the absorption cross sections of NO₂ at the two wavelengths (Table 1).

There is a large difference in the formation ratio of NO from NO₂ between the two lamps, as shown in Figure 4. The formation ratio of NO at 5 min photoirradiation is nearly the same value of $\approx 5\%$ for the two lamps. However, after 10 min photoirradiation it increases to 8–13% at 146 nm in the 5–30 min range. On the other hand, it decreases to zero in the 20–30 min range at 172 nm. In our previous study, we found

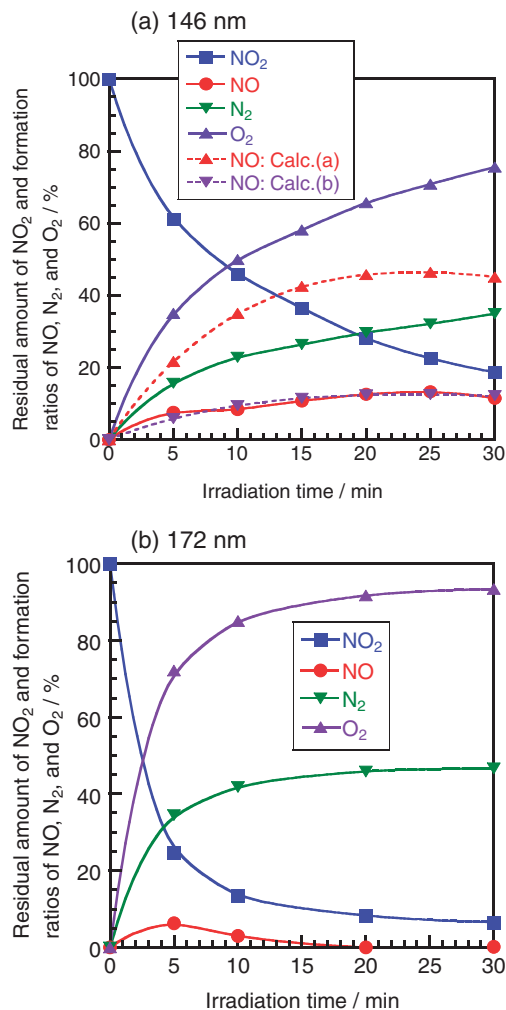
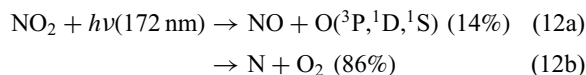


Figure 4. Dependence of the residual amount of NO₂ and the formation ratios of NO, N₂, and O₂ on the irradiation time in N₂, when (a) 25 mW cm⁻² Kr₂ and (b) 50 mW cm⁻² Xe₂ excimer lamps were used. The formation ratios of N₂ and O₂ were obtained from mass balance. The initial NO₂ concentration was 1000 ppm. Dotted curves were obtained assuming the branching ratio of reaction 13a in the consecutive reaction 14 to be 100% (Calc. (a)) and 27% (Calc. (b)).

that only 14% of NO₂ is decomposed to NO + O at 172 nm and the rest is dissociated to N + O₂ on the basis of kinetic analysis in N₂.¹⁵



We have examined the relative contribution of the two processes at 146 nm from a similar kinetic analysis.



Here, the relation $k_2 = k_{2a} + k_{2b}$ holds. At first, we assumed a simple consecutive reaction in the 146 nm photolysis of NO₂, where the branching ratio of reaction 13a is 100%.



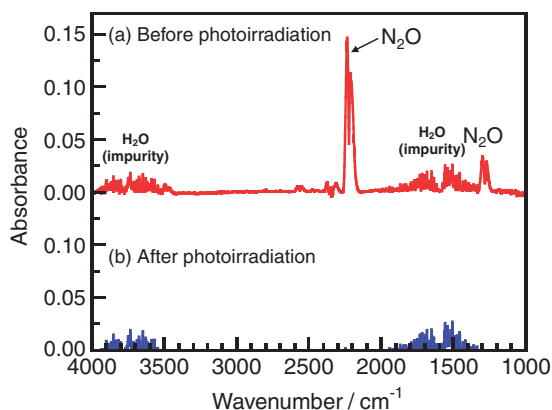


Figure 5. FTIR spectra of N₂O (100 ppm) in N₂ (a) before and (b) after 25 mW cm⁻² Kr₂ excimer lamp irradiation for 30 min.

Then, the concentration of NO was calculated as a function of irradiation time using k_1 and k_2 values obtained in this study. Figure 4a (broken line: Calc.(a)) shows the calculated NO concentrations at various irradiation times. It should be noted that the calculated NO concentrations are much higher than the observed ones. On the basis of this fact, not only reaction 13a but also reaction 13b must participate in the photolysis of NO₂ at 146 nm. In the presence of process 13b, the concentration of NO is given by

$$[\text{NO}] = k_{2a} / \{k_1 - (k_{2a} + k_{2b})\} [\exp\{-(k_{2a} + k_{2b})t\} - \exp(-k_1 t)] [\text{NO}_2]_0 \quad (15)$$

When various k_{2a} and k_{2b} values were used to reproduce the experimental data, the best fit curve was obtained at $k_{2a} = 2.4 \times 10^{-4} \text{ s}^{-1}$ and $k_{2b} = 6.6 \times 10^{-4} \text{ s}^{-1}$, as shown in Figure 4a (Calc. (b)). Therefore, the branching ratios of reactions 13a and 13b were estimated to be 27 and 73%, respectively. This shows that the direct dissociation of NO₂ to N + O₂ occurs significantly at 146 nm, as in the case of the photolysis of NO₂ at 172 nm.¹⁵ On the basis of our data for NO₂ and NO photolysis at 146 and 172 nm, a major reason for the larger formation ratio of NO from NO₂ at 146 nm than that at 172 nm can be explained by the fact that the removal rate of NO at 146 nm ($k_1 = 5.4 \times 10^{-4} \text{ s}^{-1}$) is smaller than that at 172 nm ($1.4 \times 10^{-3} \text{ s}^{-1}$) by a factor of 2.6.

N₂O Removal in N₂. Figures 5a and 5b show FTIR spectra of N₂O (100 ppm) before and after 146 nm photoirradiation. Since the absorption coefficient of N₂O for IR light is large, reliable experiments at low concentration were possible. After photoirradiation for 30 min, N₂O peaks at 2220 and 1285 cm⁻¹ disappear, and no peaks of NO and NO₂ are observed. Similar FTIR spectra of N₂O were obtained before and after 172 nm photoirradiation. Figure 6a shows the dependence of the residual amount of N₂O and the formation ratios of N₂ and O₂ on the irradiation time of the 25 mW cm⁻² 146 nm Kr₂ lamp. For comparison corresponding data for the 50 mW 172 nm Xe₂ lamp are shown in Figure 6b. It should be noted that the residual amount of N₂O at 146 nm rapidly decreases to 10, 1.6, and 0% with increasing irradiation time to 10, 20, and 30 min, respectively. On the other hand, that at 172 nm slowly decreases to 80, 62, and 48% for the same irradiation times.

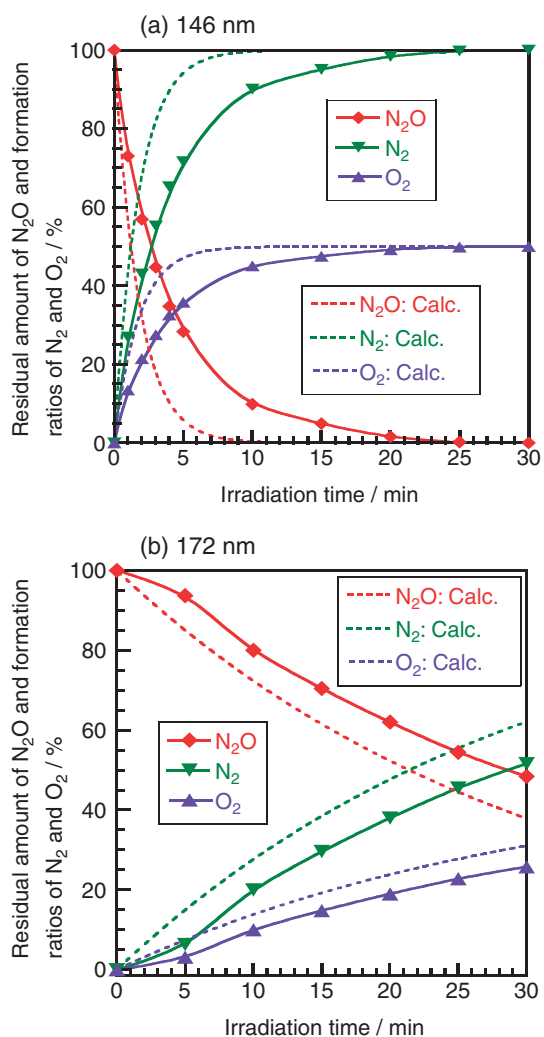


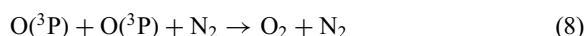
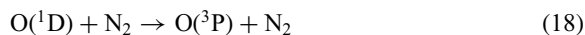
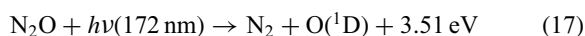
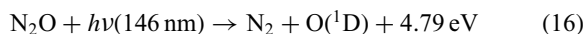
Figure 6. Dependence of the residual amount of N₂O and the formation ratios of N₂ and O₂ on the irradiation time in N₂, when (a) 25 mW cm⁻² Kr₂ and (b) 50 mW cm⁻² Xe₂ excimer lamps were used. The formation ratios of N₂ and O₂ were obtained from mass balance. The initial N₂O concentration was 100 ppm. Dotted curves were obtained from model calculation using data given in Tables 1 and 2.

From slopes of plots of $\ln([\text{N}_2\text{O}]/[\text{N}_2\text{O}]_0)$ vs. irradiation time in the 0–30 min range, the removal rates of N₂O at 146 and 172 nm, defined as k_3 , were evaluated to be 3.7×10^{-3} and $4.2 \times 10^{-4} \text{ s}^{-1}$, respectively. The correlation kinetic coefficients (R^2) of k_3 values in the linear least square plots were 0.983 at 146 nm and 0.996 at 172 nm. It should be noted that the removal rate of N₂O at 146 nm is 21 times faster than that at 172 nm, taking account of photon fluxes of the two lamps.

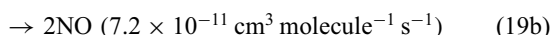
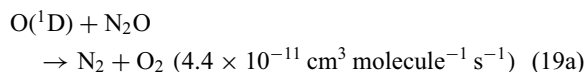
The absorption cross section of N₂O at 146 nm is 65 times larger than that at 172 nm (Table 1). In order to examine the relative contribution of N₂O and N₂ for the absorption of the 146 nm light, the $E_{\text{N}_2\text{O}}/(E_{\text{N}_2\text{O}} + E_{\text{N}_2})$ and $E_{\text{N}_2}/(E_{\text{N}_2\text{O}} + E_{\text{N}_2})$ values were evaluated using eq 4 and known σ_i and N_i values. They are 16 and 84%, respectively. Thus, we can expect that there exists a large contribution of the absorption of N₂ in the decomposition of N₂O at 146 nm under our experimental conditions. This is a major reason why the removal rate of N₂O

at 146 nm is not so fast as expected from its large absorption cross section.

On the basis of our FTIR data, it is reasonable to assume that N₂O is efficiently converted to N₂ and O₂ due to VUV photolysis of N₂O (reactions 16 and 17) and subsequent secondary reactions 18 and 8.^{19–22}



NO may be produced through fast secondary O(¹D) + N₂O reaction via process 19b.^{21,22}



However, under our conditions, the concentration of N₂O was sufficiently low (≤ 100 ppm) to suppress the O(¹D) + N₂O reaction, and NO is dominantly decomposed to N₂ and O₂ under VUV photolysis. Thus, the formation ratio of NO is negligibly small.

In order to confirm the validity of the above explanation for the VUV photolysis of N₂O in N₂ atmosphere, the residual amount of N₂O and the formation ratios of products were calculated using a similar simulation model to that used for the 193 nm ArF laser photolysis of N₂O.^{10,13} The photolysis of N₂O by the 146 and 172 nm excimer lamp starts from processes 16 and 17. The quantum yield of O(¹D) in processes 16 and 17 is known to be 1.0 in the 140–175 nm region.²² Although we used a continuous wave (CW) lamp, we applied a simulation model used for pulse laser. In the model calculations, first we calculated the total number of photons irradiated to the photolysis chamber per a unit time using irradiance of the lamp, the irradiation area of the lamp, and the one-photon energy of the 146 or 172 nm light. We assumed that our lamp operates as CW pulses with a pulse width of 10 ms (100 Hz). Then the number of photons absorbed by each molecule within 10 ms and concentrations of N₂O and products after 10 ms were calculated using five photochemical processes and their absorption cross sections at 146 nm listed in Table 1 and eighteen two-body and three-body reactions given in Table 2.^{19–22} Although the total absorption cross section of NO is known at 146 and 172 nm, little information has been reported on branching fractions of products and their electronic-state distributions. In the simulation, we assumed the following photolysis processes at 146 and 172 nm: NO → N + O(³P). When the pulse width was changed to 1 ms, similar data were obtained. Thus, the pulse width of 10 ms is sufficiently short in our simulation. The simulation data are shown in Figures 6a and 6b by dotted lines. In both cases, N₂O is removed more rapidly in the model calculation than the experimental observation. The deviation between the calculated and experimental data at 146 nm is larger than that at 172 nm. The length of our photolysis chamber is 23 cm. In our 146 nm photolysis experiments in N₂ at atmospheric pressure, incident photons lose their initial energy exponentially along the light path in the chamber due to the absorption by N₂ and attenuate

Table 2. Possible Reactions of O(¹D,³P), N(⁴S), and NO with Atoms and Molecules Induced by 146 and 172 nm Photolysis of N₂O

Reactions	Reaction number	Rate coefficients for two-body and three-body reactions (cm ³ molecule ⁻¹ s ⁻¹ and cm ⁶ molecule ⁻² s ⁻¹) (Refs. 21 and 22)
O(¹ D) + N ₂ O → N ₂ + O ₂	19a	4.4 × 10 ⁻¹¹
→ 2NO	19b	7.2 × 10 ⁻¹¹
→ O(³ P) + N ₂ O	19c	4.0 × 10 ⁻¹²
O(¹ D) + N ₂ → O(³ P) + N ₂	18	2.6 × 10 ⁻¹¹
O(¹ D) + O ₂ → O(³ P) + O ₂	20	4.0 × 10 ⁻¹¹
O(¹ D) + NO → O(³ P) + NO	21a	4.0 × 10 ⁻¹¹
→ N(⁴ S) + O ₂	21b	1.2 × 10 ⁻¹⁰
O(¹ D) + O ₃ → O ₃ + O	22a	2.41 × 10 ⁻¹⁰
→ 2O ₂	22b	1.2 × 10 ⁻¹⁰
→ O ₂ + 2O(³ P)	22c	1.2 × 10 ⁻¹⁰
O(¹ D) + NO ₂ → NO + O ₂	23a	3.01 × 10 ⁻¹⁰
→ NO ₂ + O(³ P)	23b	1.6 × 10 ⁻¹⁰
O(³ P) + O ₂ + N ₂ → O ₃ + N ₂	24	5.7 × 10 ⁻³⁴
O(³ P) + O ₂ + O ₂ → O ₃ + O ₂	25	6.2 × 10 ⁻³⁴
O(³ P) + O(³ P) + N ₂ → O ₂ + N ₂	8	4.82 × 10 ⁻³³
O(³ P) + O(³ P) + O ₂ → O ₂ + O ₂	26	1.0 × 10 ⁻³²
O(³ P) + NO + N ₂ → NO ₂ + N ₂	10	1.0 × 10 ⁻³¹
O(³ P) + NO + O ₂ → NO ₂ + O ₂	27	8.6 × 10 ⁻³²
O(³ P) + O ₃ → 2O ₂	28	8.0 × 10 ⁻¹⁵
O(³ P) + NO ₂ → NO + O ₂	29	1.05 × 10 ⁻¹¹
N(⁴ S) + N(⁴ S) + N ₂ → N ₂ + N ₂	7	1.38 × 10 ⁻³³
N(⁴ S) + NO → N ₂ + O(³ P)	9	2.92 × 10 ⁻¹¹
N(⁴ S) + NO ₂ → N ₂ O + O(³ P)	30a	1.21 × 10 ⁻¹¹
→ NO + NO	30b	7 × 10 ⁻¹²
→ N ₂ + O ₂	30c	2.12 × 10 ⁻¹²
2NO + O ₂ → 2NO ₂	11	1.93 × 10 ⁻³⁸

to only 15% at the end of the chamber at 146 nm. This strong attenuation of incidence photons at 146 nm may be a major reason for the observed slower removal rate of N₂O than that predicted from the model calculation.

N₂O Removal in N₂/O₂ Mixtures. For the practical application of the photochemical removal of N₂O, effects of O₂ must be examined because O₂ is generally present in exhausted gases. We have studied effects of O₂ in N₂/O₂ mixtures in the O₂ concentration range of 0–30%. Figures 7a and 7b show FTIR spectra observed before and after 146 nm photolysis of N₂O (100 ppm) in an N₂/O₂ mixture (O₂ 20%). Before photolysis, N₂O peaks are observed at 2220 and 1285 cm⁻¹. After 10 min photoirradiation, the N₂O peak at 2220 cm⁻¹ becomes weak by only about 5% and very strong O₃ peaks are observed. No other products such as NO, NO₂, and N₂O₅ were observed. Similar FTIR spectra were observed at 146 nm photoirradiation in N₂/O₂ mixtures (20 and 30% O₂) and at 172 nm photoirradiation in N₂/O₂ mixtures (10–30% O₂). These data imply that N₂O is dominantly converted to N₂ and O₂ in N₂/O₂ mixtures under 146 and 172 nm photoirradiation under our conditions. O₃ is produced from VUV photolysis of O₂ followed by three-body recombination reactions.^{19,21–23}

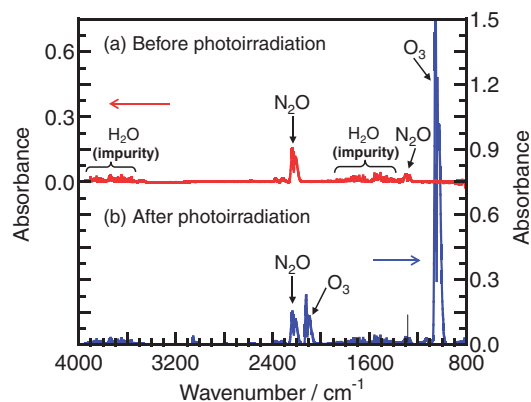
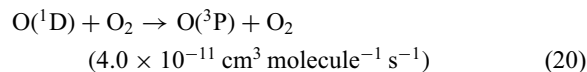
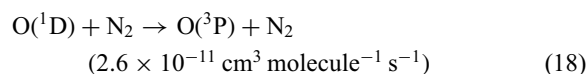
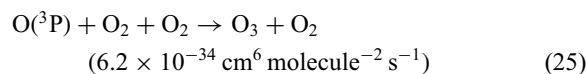
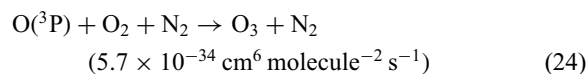
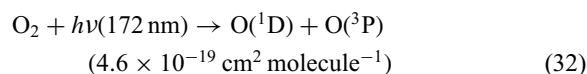
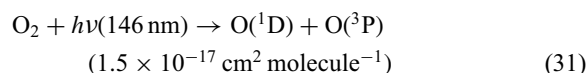


Figure 7. FTIR spectra of N₂O (100 ppm) in an N₂/O₂ (O₂ 20%) mixture (a) before and (b) after 25 mW cm⁻² Kr₂ excimer lamp irradiation for 30 min.



Figures 8a and 8b show the dependence of the residual amount of N₂O and the concentration of O₃ on the concentration of O₂ in N₂/O₂ mixtures in the 0–30% range after 10 min photoirradiation at 146 and 172 nm, respectively. Since the removal of N₂O in N₂ obeys well first-order decay in the 0–10 min range, we observed the residual amount of N₂O and the concentration of O₃ in N₂/O₂ mixtures after photoirradiation for 10 min. In Figure 8a, after the residual amount of N₂O rapidly increases from 16 to 79% with increasing the O₂ concentration from 0 to 1%, it increases from 79 to 90% in the 1–5% range and becomes 92–96% in the 5–30% range. The concentration of O₃ increases from 0 to ≈0.55% in the O₂ concentration range of 0–10% and becomes nearly constant above that. On the other hand, when a high-power 172 nm lamp was used, the residual amount of N₂O increases from 16 to 68% and the concentration of O₃ increases from 0 to 6.2% with increasing O₂ concentration from 0 to 30%, as shown in Figure 8b. These results indicate that the conversion of N₂O decreases more rapidly by the addition of O₂ at 146 nm. The σ_{146} value of O₂ is 2.3 times larger than that of N₂O and the concentration of O₂ is 100 times higher than that of N₂O even at an O₂ concentration of 1% in an N₂/O₂ mixture. Therefore, 97.4% of photons are initially absorbed by O₂ in the presence of O₂ (1%). Under such conditions, the removal of N₂O proceeds through the O(¹D) + N₂O reaction 19 in N₂/O₂ mixtures. Although the $\sigma_{146}/\sigma_{172}$ ratio for O₂ is 33, the

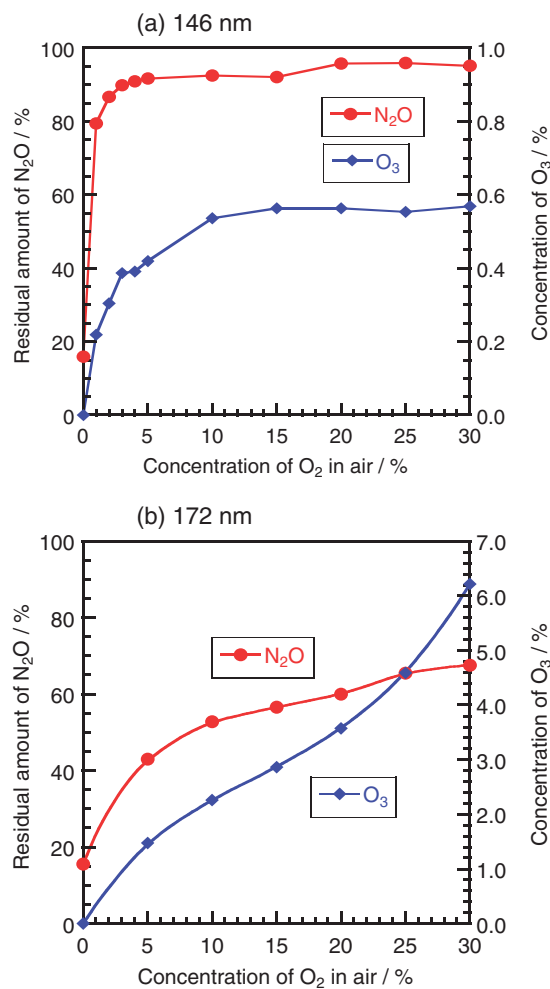


Figure 8. Dependence of the residual amount of N₂O and the concentration of O₃ on the concentration of O₂ in N₂/O₂ mixtures after 10 min photoirradiation of (a) 25 mW cm⁻² Kr₂ and (b) 300 mW cm⁻² Xe₂ excimer lamps. The initial N₂O concentration was 100 ppm.

concentrations of O(³P) and O(¹D) resulting from 146 nm photolysis of O₂ → O(³P) + O(¹D)²³ are expected to be lower than those at 172 nm under our conditions, because the observed concentration of O₃ resulting from the three-body O(³P) + O₂ + M (M = N₂ and O₂) reactions at 146 nm is lower than that at 172 nm. The lower concentration of O(¹D) at 146 nm is a major reason for the slower removal rate of N₂O at 146 nm than that at 172 nm in the presence of O₂.

Conclusion

The photolysis of NO, NO₂, and N₂O in N₂ have been studied using a 146 nm excimer lamp to develop a new photochemical removal process for NO_x and N₂O at atmospheric pressure without using any catalysts. It was found that 66% of NO (1000 ppm) was converted to N₂ (24%), O₂ (34%), and NO₂ (19%), whereas 81% of NO₂ (1000 ppm) was converted to N₂ (35%), O₂ (76%), and NO (11%) in the batch system after 30 min photoirradiation. The removal rates of NO and NO₂ at 146 nm were 11 and 36% slower than those at 172 nm, respectively. The differences in the removal rates were

discussed in terms of absorption coefficients at each wavelength and effects of photoabsorption by N₂ at 146 nm. Our results indicate that 146 nm photolysis has no great advantage over 172 nm photolysis for application to the removal of NO_x. However, we found that the 146 nm photolysis is effective for N₂O removal under N₂ in the absence of O₂. The removal rate of N₂O at 146 nm was 21 times faster than that at 172 nm. No emission of NO and NO₂ was observed.

In this work, we used a head-on type excimer lamp. A disadvantage of this type of lamp is that the irradiation area of the lamp is restricted near the quartz window. Therefore, the contact area between the light and gases is small. If a side-on 146 nm excimer lamp is developed, the contact area between the light and gases will be large, so that a higher conversion of NO_x and N₂O to N₂ and O₂ will be obtained. This will be one way for the enhancement of the removal rates of NO_x and N₂O under VUV photolysis. Thus, the rapid development of a side-on 146 nm excimer lamp is required for this purpose.

This work was partly supported by NEDO and the Joint Project of Chemical Synthesis Core Research Institutions.

References

- 1 D. J. Jacob, *Introduction to Atmospheric Chemistry*, Princeton Univ. Press, Princeton, NJ, **1999**.
- 2 *Acid Rain*, US Environmental Protection Agency, <http://www.epa.gov/acidrain/>.
- 3 *Climate Change 2001*, Working Group I, The Scientific Basis, http://www.grida.no/climate/ipcc_tar/wg1/index.htm.
- 4 EPA, *Inventory of U. S. Greenhouse Gas Emissions and Sinks: 1990–2003*, U.S. Environmental Protection Agency, <http://yosemite.epa.gov/oar/globalwarming.nsf/>.
- 5 R. M. Heck, R. J. Farrauto, S. T. Gulati, *Catalytic Air Pollution Control: Commercial Technology*, Wiley-Interscience, Weinheim, **2002**.
- 6 S. Roy, A. Marimuthu, M. S. Hegde, G. Madras, *Appl. Catal., B* **2007**, *71*, 23.
- 7 N. Nejar, M. Makkee, M. J. Illán-Gómez, *Appl. Catal., B* **2007**, *75*, 11.
- 8 J. R. Theis, E. Gulari, *Appl. Catal., B* **2007**, *75*, 39.
- 9 P. S. S. Reddy, N. Pasha, M. G. V. C. Rao, N. Lingaiah, I. Suryanarayana, P. S. S. Prasad, *Catal. Commun.* **2007**, *8*, 1406.
- 10 M. Tsuji, J. Kumagae, T. Tsuji, T. Hamagami, *J. Hazard. Mater.* **2004**, *108*, 189.
- 11 M. Tsuji, K. Noda, H. Sako, T. Hamagami, T. Tsuji, *Chem. Lett.* **2005**, *34*, 496.
- 12 M. Tsuji, H. Sako, K. Noda, M. Senda, T. Hamagami, T. Tsuji, *Chem. Lett.* **2005**, *34*, 812.
- 13 M. Tsuji, H. Sako, M. Senda, K. Noda, T. Hamagami, M. Kawahara, T. Tsuji, in *Focus on Hazardous Materials Research*, ed. by L. G. Mason, Nova Science Publishers, New York, **2007**, Chap. 4, p. 143.
- 14 M. Tsuji, M. Kawahara, M. Senda, K. Noda, *Chem. Lett.* **2007**, *36*, 376.
- 15 M. Tsuji, M. Kawahara, K. Noda, M. Senda, H. Sako, N. Kamo, T. Kawahara, K. S. N. Kamarudin, *J. Hazard. Mater.* **2009**, *162*, 1025.
- 16 M. Tsuji, M. Kawahara, M. Senda, N. Kamo, M. Kawahara, N. Hishinuma, *Eng. Sci. Rep., Kyushu Univ.* **2008**, *30*, in press.
- 17 M. Tsuji, N. Kamo, M. Senda, M. Kawahara, T. Kawahara, N. Hishimura, *Jpn. J. Appl. Phys.*, in press.
- 18 M. Tsuji, K. Nakano, J. Kumagae, T. Matsuzaki, T. Tsuji, *Surf. Coat. Tech.* **2003**, *165*, 296.
- 19 H. Okabe, *Photochemistry of Small Molecules*, John Wiley & Sons, New York, **1978**.
- 20 S. G. Lias, J. E. Bartmess, J. F. Liebman, J. L. Holmes, R. D. Levin, W. G. Mallard, *J. Phys. Chem. Ref. Data*, **1988**, *17*, Suppl. 1, 1. Updated data were obtained from NIST Standard Ref. Database, No. 69, June 2005, <http://webbook.nist.gov/chemistry>.
- 21 R. Atkinson, D. L. Baulch, R. A. Cox, R. F. Hampson, Jr., J. A. Kerr, M. J. Rossi, J. Troe, *J. Phys. Chem. Ref. Data*, **1997**, *26*, 1329. Updated data were obtained from NIST Chemical Kinetics Database on the Web, *Standard Reference Database 17, Version 7.0 (Web Version)*, Release 1.4.1, <http://kinetics.nist.gov/kinetics/index.jsp>.
- 22 IUPAC Gas Kinetic Data Evaluation, *Summary Table of Kinetic Data*, June **2006**, <http://www.iupac-kinetic.ch.cam.ac.uk>.
- 23 J. B. Nee, P. C. Lee, *J. Phys. Chem. A* **1997**, *101*, 6653.